Volume 6 | Number 23 | 7 December 2022

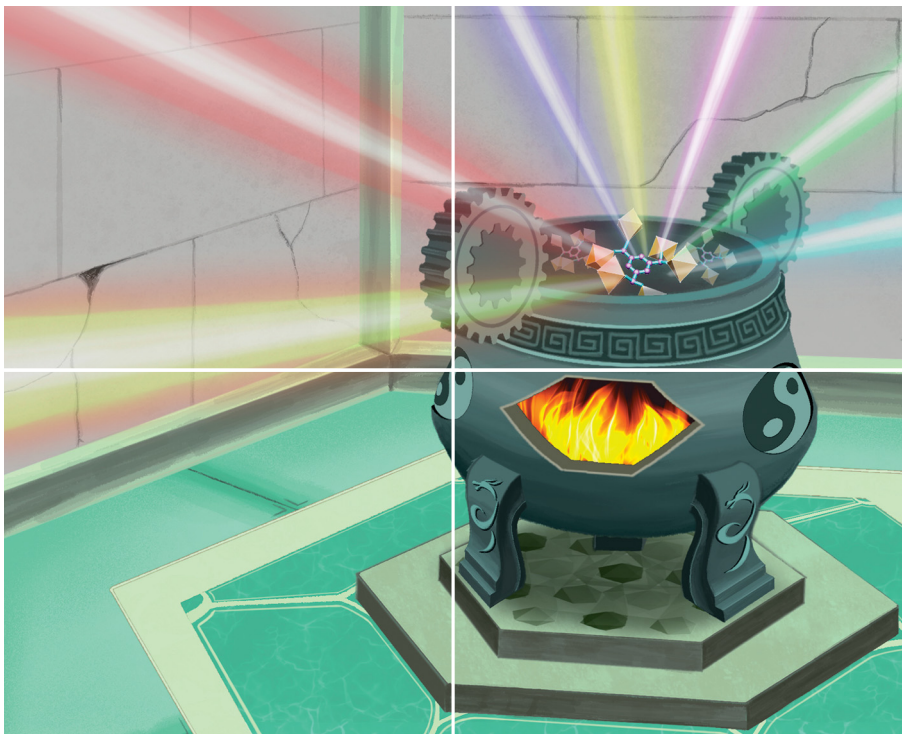

MATERIALS CHEMISTRY

FRONTIERS

CCS 中国化学会 CHINESE CHEMICAL SOCIETY

ICCAS 1956

ROYAL SOCIETY OF CHEMISTRY

rsc.li/frontiers-materials

MATERIALS CHEMISTRY FRONTIERS

RESEARCH ARTICLE

View Article Online
View Journal | View Issue

Cite this: *Mater. Chem. Front.*, 2022, **6**, 3504

Mechano-thermochemical synthesis of rare-earth metal–organic frameworks with solvent-free coordination for visible and near-infrared emission†

Jiaqiang Liu,‡[abc] Yifu Chen,‡[abc] Xin Su‡[abc] and Junbo Gong *[abc]

Rare earth metal–organic frameworks are considered as one emerging class of materials with extraordinary photoluminescence functions. However, the coordination of solvent molecules, due to their intrinsic high coordination numbers, leads to non-radiative multiphoton relaxation, which impairs their luminescence. Therefore, in this contribution, we propose a mechano-thermochemical method as a universal approach towards achieving solvent-free rare-earth metal–organic frameworks. A novel series of solvent-free rare-earth metal–organic frameworks named TJU-66 has been synthesised, exhibiting a (3,6)-c net zxc topology with a rare 6,6 coordination shape, and presenting high stabilities. Isostructural mixed metal–organic frameworks have been created by doping with rare earth ions to further improve the luminescence, reflected in the extremely high quantum yields and fluorescence lifetimes. It is worth noting that the wavelengths of different mixed metal–organic frameworks cover the whole region of visible and near-infrared light. Furthermore, by doping with Sc, the fluorescence lifetime of the Yb-based MOFs could be greatly improved up to 43.1 μs, which is so far the highest value of Yb-based MOFs. Our series of TJU-66 materials has not only replenished the existing library of luminescent metal–organic frameworks, but also, the mechano-thermochemical method highlighted in this work may provide a general method for the future development of solvent-free materials with exclusive functions.

Received 19th August 2022,
Accepted 8th October 2022

DOI: 10.1039/d2qm00839d

rsc.li/frontiers-materials

Introduction

Metal–organic frameworks (MOFs) are a class of advanced crystalline materials with tunable structures and designable functions, formed through the coordination-driven self-assembly of metal ions/clusters and organic linkers in periodic arrays, possessing great potential in various application areas, thus cherished by both chemists and materials scientists.[1–8] A characteristic group of MOFs with rare earth metal cations as framework nodes is named rare earth metal–organic frameworks (RE-MOFs).[9,10] The rare earth metal cations shall not only structurally provide the diversity of coordination modes toward abundant topological networks, but functionally generate unique advances (characteristic narrow emission bands, long luminescence lifetimes, and high resistance to photobleaching, for example) from their special 4f electron configurations.[9,11–14] Therefore, great efforts have been made in structural modulation of the topological framework as well as doping with other rare earth metal ions for an improvement of the luminescence; however, to design and construct RE-MOFs with strong emission intensity and long fluorescence lifetimes is still challenging.

Relative to other transition metal MOFs, the large radii of rare earth metal ions always result in a higher coordination number,[15] leading to the common occurrence that solvent molecules coordinate to the rare earth metal ions in RE-MOFs. Unfortunately, the luminescence of RE-MOFs can be easily quenched by high-energy vibrational groups (*e.g.*, O–H, C–H, and N–H) of solvent molecules (*e.g.*, water, methanol, and dimethyl formamide) near the rare earth metal ions owing to the non-radiative multiphoton relaxation, reflected in the great weakening of luminescence in both the visible and near-infrared (NIR) regions, but is more pronounced in the NIR

[a] *State Key Laboratory of Chemical Engineering, School of Chemical Engineering and Technology, Tianjin University, Weijin Road 92, Tianjin, 300072, P. R. China. E-mail: junbo_gong@tju.edu.cn*
[b] *Collaborative Innovation Center of Chemistry Science and Engineering, Weijin Road 92, Tianjin, P. R. China*
[c] *Haihe Laboratory of Sustainable Chemical Transformations, Tianjin, 300192, P. R. China*

† Electronic supplementary information (ESI) available: Experimental details, photoluminescence spectra, scanning electron microscopy, energy-dispersive X-ray spectrometry and powder X-ray diffraction. CCDC 2154763 and 2154761. For ESI and crystallographic data in CIF or other electronic format see DOI: https://doi.org/10.1039/d2qm00839d

‡ These authors contributed equally to this work.

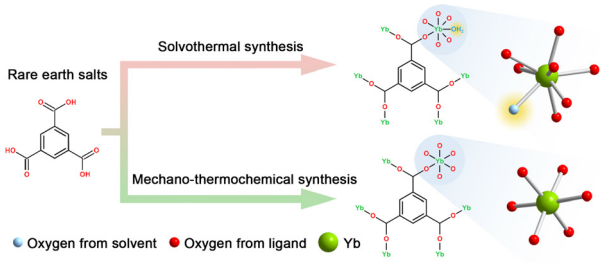

Fig. 1 Illustration of the effect of different synthesis methods on the presence or absence of coordinated solvent molecules in RE-MOFs.

regions.[12,16] Thus, how to avoid solvent molecular coordination is the key to achieving high quantum yields and long fluorescence lifetimes in RE-MOFs.

In contrast to the existing system-specific attempts of selecting a specific ligand to exclude the ligand solvents,[16,17] we herein propose a new concept, a mechano-thermochemical method, as a universal approach towards achieving solvent-free RE-MOFs. It is well-known that solvothermal synthesis is the most classic method in MOFs, that can produce highly crystalline crystals, but may result in excessive solvent coordination[18–20] (Fig. 1). Furthermore, mechanochemical synthesis serves as a versatile tool for efficient, environmentally friendly construction of MOFs, but results in the low crystallinity of products. Our mechano-thermochemical approach could integrate the advantages of both the solvothermal and mechanochemical methods, and complement the deficiencies of them, obtaining solvent-free coordination products with high crystalline properties (Fig. 2).

In this work, RE-MOFs are focused on as a case study to highlight the advantages of the mechano-thermochemical method in the preparation of solvent-free MOF materials. The synthetic RE-MOFs exhibited a unique 6,6 coordination shape, hence the name TJU-66. TJU is an abbreviation for Tianjin University. Precise crystallographic structural information was directly resolved using powder X-ray diffraction patterns, assisted by photoluminescence emission properties and Fourier transform infrared absorption spectra. A series of TJU-66 isostructural mixed metal–organic framework materials in solvent-free coordination mode have been modulated by rare earth metal doping to ensure excellent visible and near infrared emission, reflecting the exclusive advantages of mechano-thermochemical synthesis. Notably, scandium (Sc) metal doping can significantly increase the fluorescence lifetimes of ytterbium (Yb)-based MOFs, which have even more potential applications in time-resolved detection.[21] In addition, it was explored that TJU-66 isomorphic MOFs exhibit exceptional thermal and water stability, ensuring the viability of the materials in practical applications.[22,23]

Solvothermal method	Mechanochemical method	Mechano-thermochemical method
High temperature	Room temperature	High temperature
High pressure	No high voltage	No high voltage
Large amounts of liquid wastes	Minimum wastes	Minimum wastes
Highly crystalline products	Possible amorphization	Highly crystalline products
Basic equipment	Special grinders	Basic equipment (basic grinders)
Pure products	Possible impurities	Pure products
Precise control of synthesis	Difficult to control synthesis precisely	Precise control of synthesis

Fig. 2 Comparison of typical solventhermal, mechanochemical, and mechano-thermochemical methods. The green parts mark advantages, the red parts mark disadvantages.

Results and discussion

Crystal structure analysis

The sharp diffraction peaks in the powder X-ray diffraction pattern indicate that the crystallinity of TJU-66 (Yb or Sc) is 100% (FWHM threshold of amorphous peaks = 3 in Fig. 3a and b), demonstrating the advantages of the mechano-thermochemical method over the traditional mechanochemical process for crystallising products.[24] Structural elucidation of TJU-66 was carried out by high-resolution powder X-ray diffraction analysis. Pattern indexing was performed based on the experimental diffraction data, and the point group of TJU-66 was determined to belong to a less symmetric triptycene (C_{3v}) with the space group $R3c$. The crystallographic structure was further demonstrated by the photoluminescence properties of Eu^{3+}, shown in Fig. S1 (ESI†).[25] Considering the connection of the metal nodes and ligands, to understand the lattice packing of TJU-66, a three-dimensional structure model was constructed using Materials Studio 6.0 software. Finally, Pawley refinements give the optimized parameters as follows: $a = b = 8.92$ Å, $c = 18.70$ Å, $\alpha = \beta = 90^\circ$, $\gamma = 120^\circ$, $R_{wp} = 7.03\%$ and $R_p = 4.43\%$ for TJU-66(Yb); $a = b = 8.69$ Å, $c = 18.63$ Å, $\alpha = \beta = 90^\circ$, $\gamma = 120^\circ$, $R_{wp} = 6.75\%$ and $R_p = 4.85\%$ for TJU-66 (Sc). Also, the calculated simulated powder pattern exactly matches the experimentally obtained peak positions (Fig. 3a and b). The crystallographic data were deposited with the Cambridge Crystallographic Data Centre (CCDC 2154763 and 2154761,† respectively)

The structural feature shows unusual 6-coordination of linkage properties, like d-block elements, which is rare in the complexes of rare-earth ions with small molecular linkers with low spatial site resistance. In the TJU-66 framework structure, each rare-earth metal centre is coordinated to six oxygen atoms of carboxylic acid groups from six different 1,3,5-benzenetricarboxylic acid ligands to form an octahedron, thus each ligand is coordinated to six rare earth metal centres.[26] This familiar octahedral shape of the bifurcated ligand is chiral, however, the entire three-dimensional network framework is non-chiral, as two chiral forms of construction are taken in assembling the network. The basic net in the MOF of octahedral metal nodes is pcu, more precisely described as the derived (3,6)-c net zxc (Fig. 3c–f).[26] In particular, the chiral ligands are connected in a non-centrosymmetric manner, thus giving the exclusive non-centrosymmetric space group $R3c$ rather than the default symmetric space group $R\bar{3}c$.[26] Rationally, the exceptional configuration of TJU-66 is fortunately due to a solvent-free synthetic environment induced self-assembly by a mechano-thermochemical method.

The topological structure types of 16 RE-MOFs (RE = La, Ce, Pr, Nd, Sm, Eu, Gd, Tb, Dy, Ho, Y, Er, Tm, Yb, Lu or Sc) synthesised by a mechano-thermochemical method were

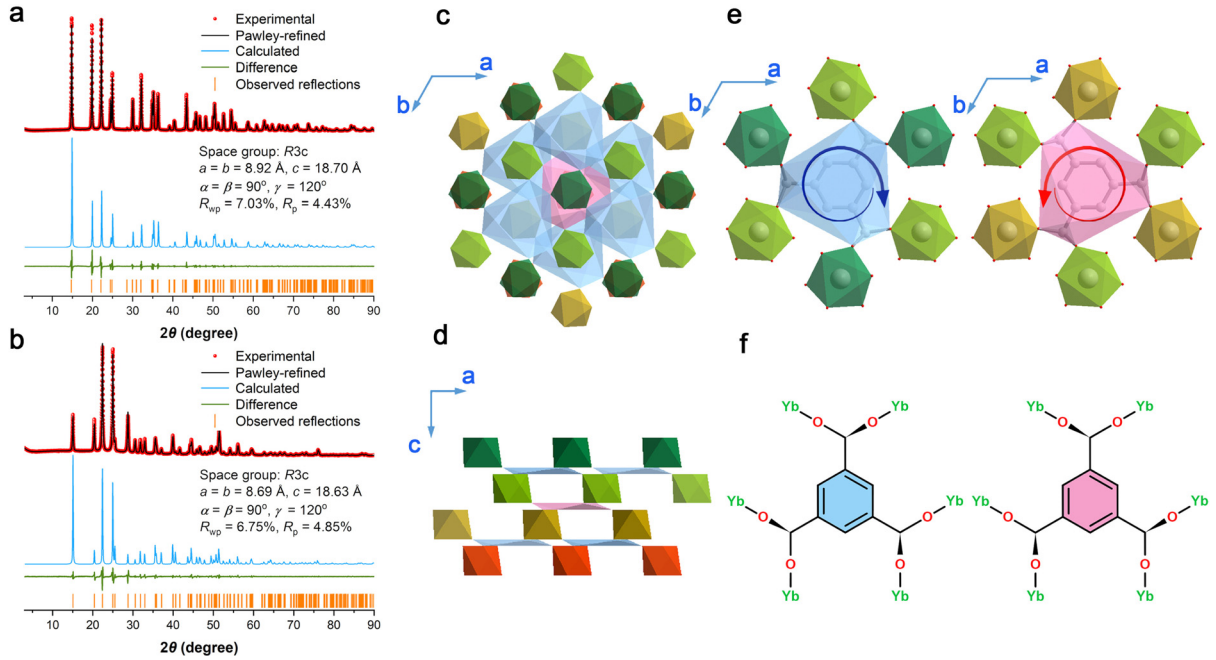

Fig. 3 The structures of TJU-66 confirmed by Pawley refinements. PXRD patterns of (a) TJU-66 (Yb) and (b) TJU-66 (Sc) with experimental data in red, Pawley-refined curves in black, calculated curves in blue, and difference plots in green. The allowed peak positions are marked as orange tics. View of TJU-66(Yb) (c) down the [00_1] direction and (d) down the [_120] direction. (e) View of the coordination of bichiral organic linkers with six unique YbO_6 polyhedra, and (f) structural formula for the coordination of bichiral organic linkers with Yb from TJU-66(Yb).

investigated, with three topological configurations appearing or disappearing in sequence as the ionic radius shrinks in the powder X-ray diffraction spectrum of Fig. 4a, demonstrating the structure-directing effects of synthetic environmental induction and lanthanide contraction.[27,28] The characteristic peaks of powder X-ray diffraction patterns for RE-MOF (RE = La, Ce, Pr, Nd, Sm, Eu, Gd, Tb or Dy) obtained correspond to La(BTC)·$6H_2O$ (CCDC 290771†)[19,20] (the characteristic peaks are marked in Fig. 4a with a yellow background and the coordinated structure is shown in Fig. 4b). The rare earth metal centre in

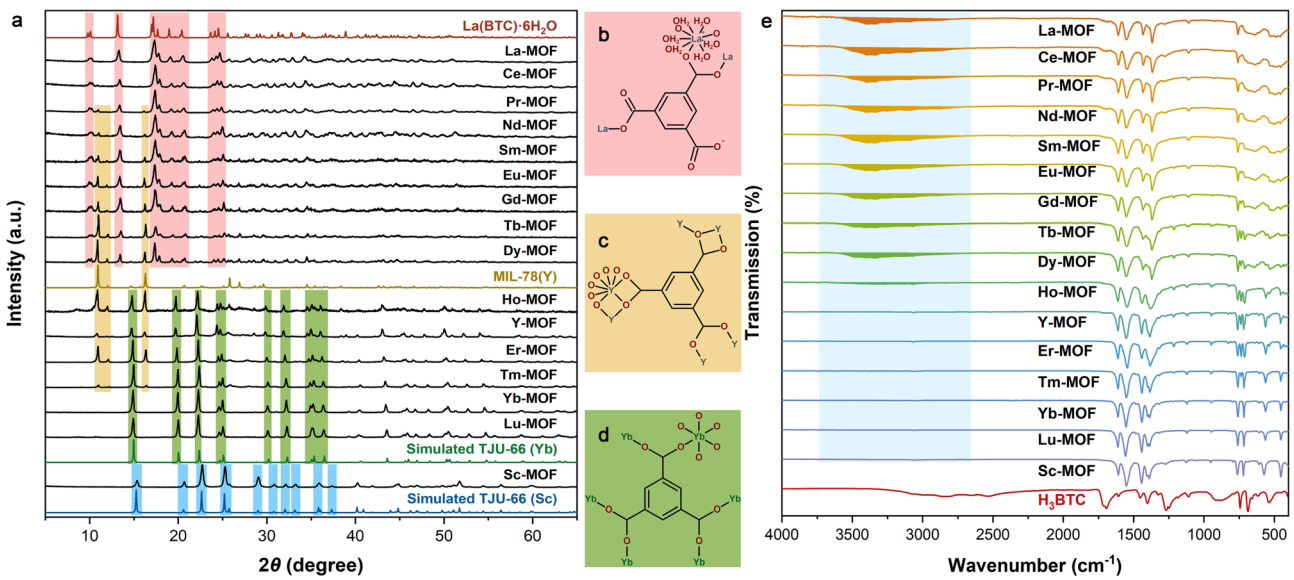

Fig. 4 Comparison of different topologies from RE-MOFs. (a) (from top to bottom) Simulated PXRD patterns of La(BTC)·$6H_2O$ with CCDC 290771,† experimental PXRD patterns of the prepared RE-MOF (RE = La, Ce, Pr, Nd, Sm, Eu, Gd, Tb or Dy), simulated PXRD pattern of MIL-78 (Y) with CCDC 1109360,† prepared RE-MOF (RE = Ho, Y, Er, Tm, Yb or Lu), simulated PXRD pattern of TJU-66 (Yb), experimental PXRD pattern of prepared Sc-MOF, and simulated PXRD pattern of TJU-66 (Sc); (b–d) Structural formulae for La(BTC)·$6H_2O$, MIL-78 (Y) and TJU-66 (Yb); (e) (from top to bottom) FTIR absorption spectra of the prepared RE-MOF (RE = La, Ce, Pr, Nd, Sm, Eu, Gd, Tb, Dy, Ho, Y, Er, Tm, Yb, Lu or Sc), and H_3BTC, respectively.

this structure is coordinated to six water molecules in addition to the carboxylic acid groups from the three ligands. Then, the components of the La(BTC)·6H_2O structure gradually decrease to disappear with lanthanide contraction, and the MIL-78(Y) (CCDC 1109360†)[29–31] (the characteristic peaks are marked in Fig. 4a with a yellow background and the coordinated structure is shown in Fig. 4c) configuration with eight-coordinated rare-earth polyhedral, in which the metal centres are not coordinated to water molecules, appears and disappears in the product RE-MOF (RE = Pr, Nd, Sm, Eu, Gd, Tb, Dy, Ho, Y, Er or Tm). Subsequently, novel solvent-free coordination TJU-66 (Yb) as well as the isostructural TJU-66 (Sc) occur in RE-MOF (RE = Ho, Y, Er Tm, Yb, Lu or Sc) (the characteristic peaks are marked in Fig. 4a with green and blue backgrounds respectively and the coordinated structure is demonstrated in Fig. 4d). Furthermore, TJU-66 (Yb) was used as an example for heat treatment times (t = 3 h, 12 h, 24 h or 48 h) to investigate the division of labour between mechanochemical and thermochemical processes in crystal nucleation and growth for the synthesis method. The topological structure characteristic peaks of the novel crystals in powder X-ray diffraction patterns were found to appear after 3 hours of heat treatment, as shown in Fig. S4 (ESI†), demonstrating that their thermochemical processes are the overwhelming contributors to crystallinity.

The Fourier transform infrared absorption spectra of RE-MOFs further confirm the solvent-free coordination structure of TJU-66. As shown in Fig. 4e, the characteristic spectral band of the O–H group in the water molecule at 3000–3500 cm^{-1} disappears as the components of the La(BTC)·6H_2O structure gradually decrease to vanish. This indicates that the MIL-78 and TJU-66 conformation do not contain coordinated or encapsulated water molecules, which is beneficial for the construction of high-performance photonic functional materials. Also fundamental is that the FTIR spectrum of H_3BTC shows the absorption at 3083 cm^{-1} (ν O–H), 1716 cm^{-1} (ν C═O) and 533 cm^{-1} (δ C═O). In contrast, the absorption spectrum of RE-MOFs, located at 1606–1545 cm^{-1} (asymmetric stretching vibration of –COO–) and 1443–1387 cm^{-1} (symmetric stretching vibration of –COO–), prove the formation of coordination bonds.

Structural stability investigation

The thermal stability of MOFs is an important parameter for their application in materials chemistry, and the TJU-66 structure possesses high stability by eliminating the perturbation of the structure and the weakening of ligand bonds by solvent stripping. The structural stability properties are explored in different atmospheres by means of *in situ* PXRD techniques and thermogravimetric analysis (TGA) using TJU-66 (Yb) as an example. The *in situ* PXRD test is carried out to collect diffraction patterns of synthesised TJU-66 (Yb) at different temperatures (multiple temperature points between 25 °C and 900 °C) in an air atmosphere, shown in Fig. 5a. The two diffraction peaks of the (104) crystal plane form of TJU-66(Yb) (2θ = 22.41°) and the (222) crystal plane form of Yb_2O_3 (2θ = 28.78°) are selected to analyse the variation in height, making the interpolation in Fig. 5a. It can be observed that the crystal structure

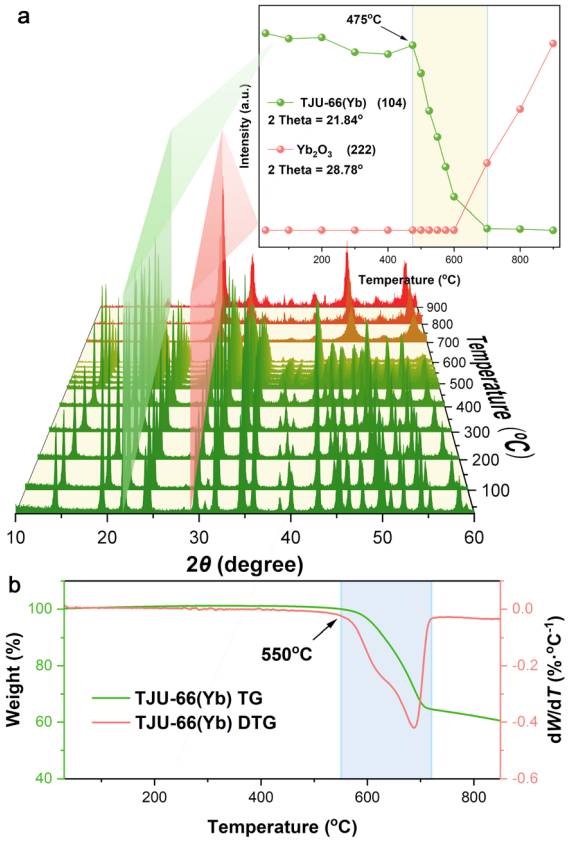

Fig. 5 Stability analysis of TJU-66. (a) *In situ* PXRD patterns of TJU-66(Yb), and the interpolation shows the variation of the two diffraction peaks of the (104) crystal plane from TJU-66(Yb) and (222) crystal plane from Yb_2O_3. (b) TGA curves registered under a dynamic N_2 atmosphere of TJU-66(Yb).

of the material starts to decompose after 475 °C and can maintain about 80% of the diffraction peak at 500 °C. Thermogravimetric analysis test under a dynamic N_2 atmosphere shows that the weight loss of TJU-66(Yb) starts at 550 °C, which further supports that it is not coordinated or encapsulated with solvent small molecules such as water. Thus, the higher weight loss temperature presents the excellent thermal stability of this crystalline material. In contrast, MOFs synthesised using the solvothermal method, which usually have solvents coordinated or presented as guests within their pores, must be removed by thermal and vacuum activation prior to application. However, solvent removal can lead to structural degradation caused by capillary forces due to the narrow pore size, which can cause crystal breakage and reduce their thermal stability.[32,33]

Photophysical property study

The high-performance photoluminescent mixed metal–organic frameworks TJU-66(RE/Sc) (RE= Sm, Eu, Tb, Dy, Yb, Nd or Er) are synthesized using the rare earth metal ion doping method. The PXRD pattern and FTIR absorption spectra show that the conformations are essentially the same as TJU-66(Sc), maintaining the solvent-free coordination structure. The doped Sc^{3+} ions are homogeneously distributed within the MOF crystal as

shown in the energy-dispersive X-ray spectrometry mapping images (Fig. S3, ESI†). The photophysical properties of single and mixed metal–organic frameworks in the solid state were characterized with the photoluminescence excitation (PLE) spectrum and visible and near infrared photoluminescence (PL) spectrum. The characterisation results follow the energy transfer mechanism proposed by Crosby and Whan for organic ligands to lanthanide ions.[34] Under UV irradiation at 300 nm, the organic ligand of TJU-66 is excited to the vibrational energy level of the first excited singlet state ($S_1 \leftarrow S_0$), and then undergoes nonradiative intersystem crossing from the singlet state S_1 to the triplet state T_1. The nonradiative transition from the triplet state to the excited state of the lanthanide ion excites the rare earth element ion by energy transfer. The radiative transitions to lower energy levels can be observed as characteristic linear photoluminescence with visible and infrared emission from TJU-66(RE/Sc) (RE = Sm, Eu, Tb, Dy, Yb or Nd) in Fig. 6c–i. However, TJU-66(Er/Sc) exhibits emission weakly in the IR II region. According to energy level analysis, the weak performance can be attributed to the fact that the triplet state energy level of BTC (23 200 cm^{-1}) is so far above that of the emitting lanthanides $E^{Er}(^4I_{13/2})$ = 6700 cm^{-1} that effective energy transfer is not possible.[16,35]

The quantum yields and fluorescence lifetimes of the near infrared emissions from TJU-66 (Yb) and TJU-66 (Yb/Sc) were measured to investigate the effect of metal doping on photophysical properties. Compared with the single-component MOF, the quantum yield of the Sc metal-doped MOF is increased by about 30%, and the fluorescence lifetime (τ_{au}) is significantly increased by nearly 4 times, from 10.9 μs to 43.1 μs (Fig. 7 and Table 1). This suggests that ion doping resolves the detrimental effect of concentration quenching on quantum yields. It also changes the environment around the Yb^{3+} ions in TJU-66 (Yb/Sc), increasing one optical centre, allowing the fluorescence lifetime to change from fitting a double to a triple exponential fit. The sensitisation process of the Yb^{3+} ions is very sensitive to this small environmental change, contributing to the longer lifetimes. Remarkably, the fluorescence lifetime of

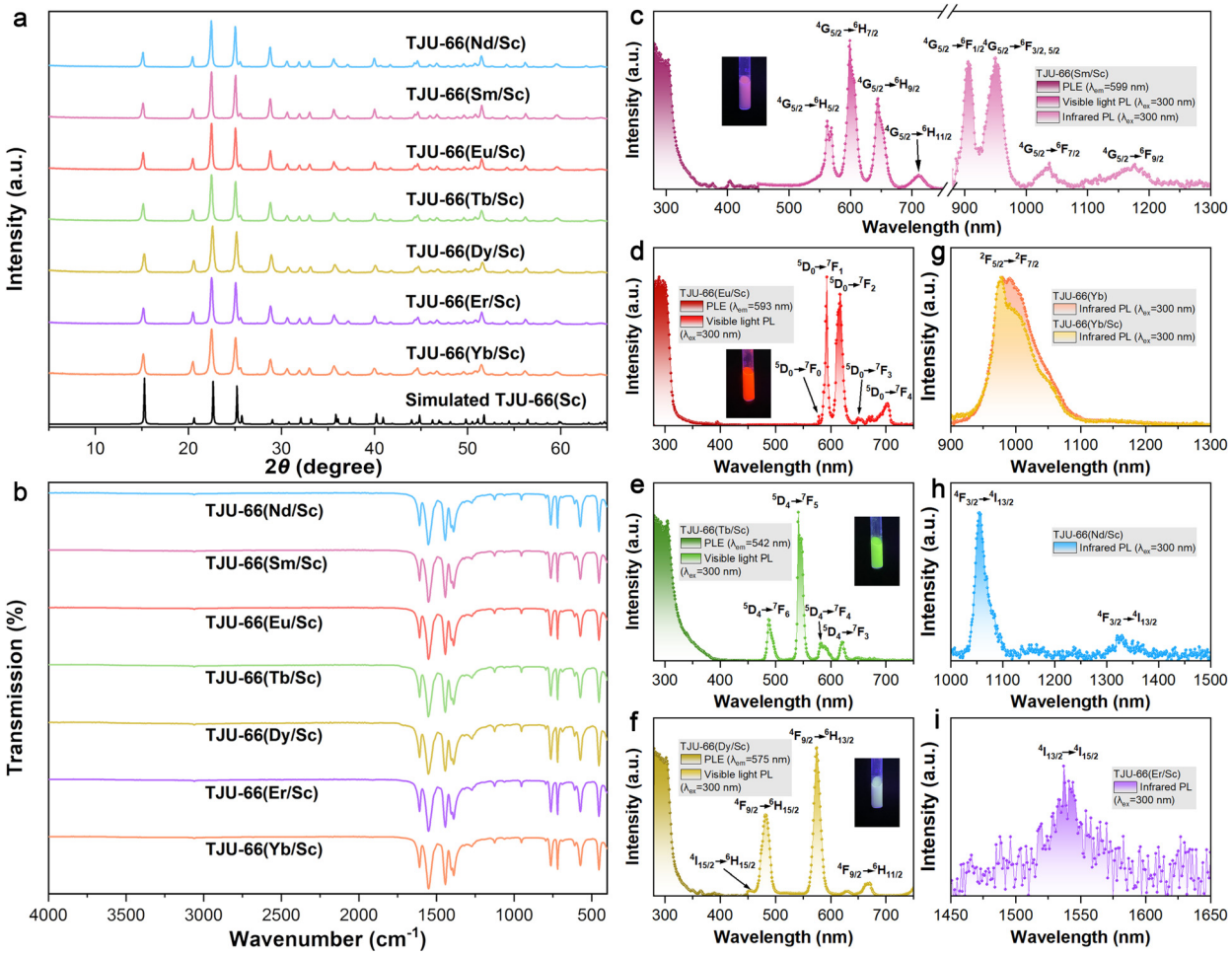

Fig. 6 Structural and photophysical property studies of mixed metal–organic frameworks. (a) (from top to bottom) experimental PXRD patterns of TJU-66(RE/Sc) (RE = Nd, Sm, Eu, Tb, Dy, Er or Yb), and simulated PXRD patterns of TJU-66(Sc). (b) (from top to bottom) FTIR absorption spectra of the prepared TJU-66(RE/Sc) (RE = Nd, Sm, Eu, Tb, Dy, Er or Yb). (c) PLE spectrum and visible and near infrared PL spectrum of TJU-66 (Sm/Sc). (b–d) PLE and visible PL spectrum of TJU-66 (RE/Sc) (RE = Eu, Tb or Dy). Near infrared PL spectrum of (e) TJU-66 (Yb), TJU-66 (Yb/Sc), (f) TJU-66 (Nd/Sc), (g) TJU-66 (Er/Sc), respectively.

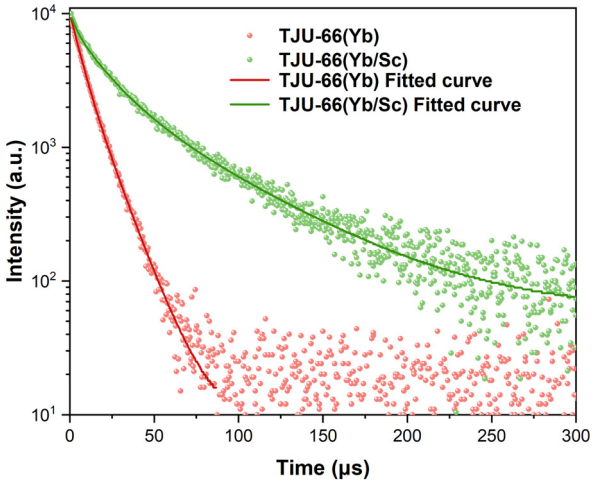

Fig. 7 Fluorescence lifetimes of TJU-66 (Yb) and TJU-66 (Yb/Sc).

Table 1 Quantum yields and luminescence lifetimes of TJU-66 (Yb) and TJU-66 (Yb/Sc)[a]

	Q^{L}_{Yb} (%)	Lifetime (μs)	
TJU-66(Yb)	1.03(2)	τ_1: 6.0(0.3) : 50.6(6.4)% τ_2: 13.1(0.3) : 49.4(7.0)%	τ_{au}: 10.9(0.3)
TJU-66(Yb/Sc)	1.32(2)	τ_1: 4.1(0.8) : 18.5(14.2)% τ_2: 18.4(1.3) : 50.9(3.8)% τ_3: 57.9(2.0) : 30.6(7.5)%	τ_{au}: 43.1(1.8)

[a] 2σ values are given in parentheses. Lifetimes measured under excitation at 300 nm.

TJU-66 (Yb/Sc) is the highest among those of the currently reported Yb-based MOFs,[16,17,36–38] indicating its potential for application in time-resolved detection.

The extraordinary water stability of the TJU-66 series materials provides them with potential for applications such as trace detection, molecular identification, potential fingerprinting, *etc.*[23,30,31] The TJU-66 (RE/Sc) (RE= Sm, Eu, Tb or Dy) with bright visible light emission was dispersed in water for 90 days. The PXRD patterns and FTIR absorption spectra show no significant changes in structure (Fig. 8a and b) and no noticeable difference in photoluminescence ability after 90 days (inset of Fig. 8a).

Conclusions

In conclusion, a mechano-thermochemical method, combining mechanical grinding and thermal treatment, is proposed to prepare solvent-free ligated RE-MOFs to avoid the reduced quantum yields and shortened lifetimes associated with non-radiative multiphoton relaxation. A novel series of solvent-free coordination metal complexes, called TJU-66, has been synthesised, exhibiting a rare 6,6 coordination shape, giving the exclusive non-centrosymmetric space group *R*3*c*. Multiple isomorphic mixed rare-earth metal organic frameworks have been

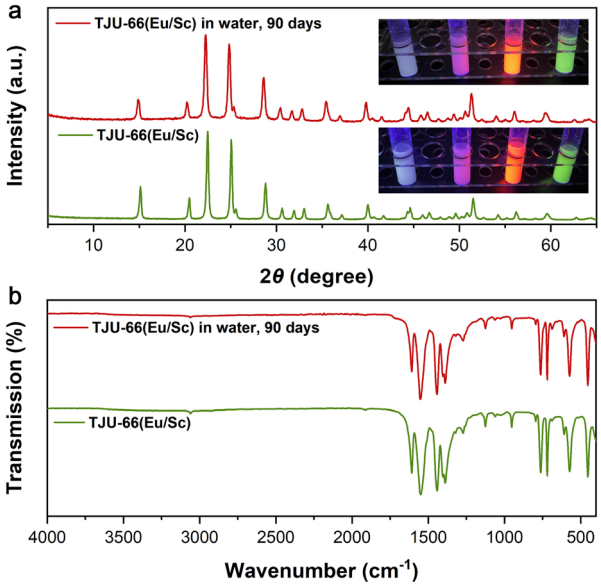

Fig. 8 Water stability analysis of TJU-66. (a) PXRD pattern and (b) FTIR absorption spectra of the original TJU-66 (Eu/Sc) and the dispersion in water for 90 days. The inset shows the photoluminescence state of the TJU-66 (RE/Sc) (RE= Sm, Eu, Tb or Dy), λ_{ex} = 254 nm.

modulated by rare-earth ion doping, with excellent visible and near-infrared emission properties. In this approach, the fluorescence lifetime of Yb-based MOFs has been greatly enhanced by the doping of Sc, up to 43.1 μs, which is to the best of our knowledge the highest value reported in Yb-based MOFs, which may have great potential for applications in time-resolved detection, fluorescence lifetime encoding, *etc.* In addition, the TJU-66 structure has been explored for its excellent thermal and water stability, ensuring the viability of isostructural functional materials for practical applications. Our findings provide a sustainable and environmentally friendly prospective due to the solvent-free synthesis of highly crystalline functional materials.

Author contributions

J. Liu and X. Su codesigned the experiments, implemented the preparation of materials, carried out the characterization tests and analyzed the experimental results. Y. Chen supervised the whole study, revised the manuscript, discussed the results and helped in drawing the figures. J. Liu, Y. Chen and X. Su contributed equally to this work. J. Gong acquired funding for the whole study. All authors commented on the manuscript.

Conflicts of interest

There are no conflicts to declare.

Acknowledgements

The authors are grateful for the financial support from the National Natural Science Foundation of China (21938009), the

Innovative Research Group Project of the National Natural Science Foundation of China (21621004), and the National Science Foundation of Tianjin City (19JCZDJC37500).

References

1 O. M. Yaghi, G. Li and H. Li, Selective binding and removal of guests in a microporous metal-organic framework, *Nature*, 1995, **378**, 703–706.
2 B. Li, H. M. Wen, Y. Cui, W. Zhou, G. Qian and B. Chen, Emerging Multifunctional Metal-Organic Framework Materials, *Adv. Mater.*, 2016, **28**, 8819–8860.
3 H. Li, M. Eddaoudi, M. O'Keeffe and O. M. Yaghi, Design and synthesis of an exceptionally stable and highly porous metal-organic framework, *Nature*, 1999, **402**, 276–279.
4 L. Rosi Nathaniel, J. Eckert, M. Eddaoudi, T. Vodak David, J. Kim, M. O'Keeffe and M. Yaghi Omar, Hydrogen Storage in Microporous Metal-Organic Frameworks, *Science*, 2003, **300**, 1127–1129.
5 Y. Chen, B. Yu, Y. Cui, S. Xu and J. Gong, Core–Shell Structured Cyclodextrin Metal–Organic Frameworks with Hierarchical Dye Encapsulation for Tunable Light Emission, *Chem. Mater.*, 2019, **31**, 1289–1295.
6 Y. Chen, B. Yu, S. Xu, F. Ma and J. Gong, Core-Shell-Structured Cyclodextrin Metal-Organic Frameworks for Programmable Cargo Release, *ACS Appl. Mater. Interfaces*, 2019, **11**, 16280–16284.
7 X. L. Lv, L. Feng, L. H. Xie, T. He, W. Wu, K. Y. Wang, G. Si, B. Wang, J. R. Li and H. C. Zhou, Linker Desymmetrization: Access to a Series of Rare-Earth Tetracarboxylate Frameworks with Eight-Connected Hexanuclear Nodes, *J. Am. Chem. Soc.*, 2021, **143**, 2784–2791.
8 B. Wang, X. L. Lv, D. Feng, L. H. Xie, J. Zhang, M. Li, Y. Xie, J. R. Li and H. C. Zhou, Highly Stable Zr(IV)-Based Metal-Organic Frameworks for the Detection and Removal of Antibiotics and Organic Explosives in Water, *J. Am. Chem. Soc.*, 2016, **138**, 6204–6216.
9 Y. Cui, Y. Yue, G. Qian and B. Chen, Luminescent functional metal-organic frameworks, *Chem. Rev.*, 2012, **112**, 1126–1162.
10 M. Pan, Y. X. Zhu, K. Wu, L. Chen, Y. J. Hou, S. Y. Yin, H. P. Wang, Y. N. Fan and C. Y. Su, Epitaxial Growth of Hetero-Ln-MOF Hierarchical Single Crystals for Domain- and Orientation-Controlled Multicolor Luminescence 3D Coding Capability, *Angew. Chem., Int. Ed.*, 2017, **56**, 14582–14586.
11 F. Saraci, V. Quezada-Novoa, P. R. Donnarumma and A. J. Howarth, Rare-earth metal-organic frameworks: from structure to applications, *Chem. Soc. Rev.*, 2020, **49**, 7949–7977.
12 S. A. Younis, N. Bhardwaj, S. K. Bhardwaj, K.-H. Kim and A. Deep, Rare earth metal-organic frameworks (RE-MOFs): Synthesis, properties, and biomedical applications, *Coord. Chem. Rev.*, 2021, **429**, 213620.
13 X.-Y. Liu, W. P. Lustig and J. Li, Functionalizing Luminescent Metal–Organic Frameworks for Enhanced Photoluminescence, *ACS Energy Lett.*, 2020, **5**, 2671–2680.
14 X.-Z. Song, S.-Y. Song and H.-J. Zhang, in *Lanthanide Metal-Organic Frameworks*, ed. P. Cheng, Springer Berlin Heidelberg, Berlin, Heidelberg, 2015, pp. 109–144, DOI: **10.1007/430_2014_160**.
15 J.-C. G. Bünzli, A.-S. Chauvin, H. K. Kim, E. Deiters and S. V. Eliseeva, Lanthanide luminescence efficiency in eight- and nine-coordinate complexes: Role of the radiative lifetime, *Coord. Chem. Rev.*, 2010, **254**, 2623–2633.
16 T. N. Nguyen, S. V. Eliseeva, A. Gładysiak, S. Petoud and K. C. Stylianou, Design of lanthanide-based metal–organic frameworks with enhanced near-infrared emission, *J. Mater. Chem. A*, 2020, **8**, 10188–10192.
17 K. A. White, D. A. Chengelis, M. Zeller, S. J. Geib, J. Szakos, S. Petoud and N. L. Rosi, Near-infrared emitting ytterbium metal-organic frameworks with tunable excitation properties, *Chem. Commun.*, 2009, 4506–4508.
18 M. Gustafsson, A. Bartoszewicz, B. Martín-Matute, J. Sun, J. Grins, T. Zhao, Z. Li, G. Zhu and X. Zou, A Family of Highly Stable Lanthanide Metal-Organic Frameworks: Structural Evolution and Catalytic Activity, *Chem. Mater.*, 2010, **22**, 3316–3322.
19 J. Liu, X. Yue, Z. Wang, X. Zhang and Y. Xu, Coumarin 7 functionalized europium-based metal-organic-framework luminescent composites for dual-mode optical thermometry, *J. Mater. Chem. C*, 2020, **8**, 13328–13335.
20 J. Liu, Y. Zhao, X. Li, J. Wu, Y. Han, X. Zhang and Y. Xu, Dual-Emissive $CsPbBr_3$@Eu-BTC Composite for Self-Calibrating Temperature Sensing Application, *Cryst. Growth Des.*, 2019, **20**, 454–459.
21 D. J. Ni, J. Zhang, Z. K. Cao, R. Li, T. F. Xu, H. W. Sang, S. Ramakrishna and Y. Z. Long, Supersensitive and reusable perovskite nanocomposite fiber paper for time-resolved single-droplet detection, *J. Hazard. Mater.*, 2021, **403**, 123959.
22 M. Ding, X. Cai and H. L. Jiang, Improving MOF stability: approaches and applications, *Chem. Sci.*, 2019, **10**, 10209–10230.
23 C. Wang, X. Liu, N. Keser Demir, J. P. Chen and K. Li, Applications of water stable metal-organic frameworks, *Chem. Soc. Rev.*, 2016, **45**, 5107–5134.
24 N. K. Singh, M. Hardi and V. P. Balema, Mechanochemical synthesis of an yttrium based metal-organic framework, *Chem. Commun.*, 2013, **49**, 972–974.
25 K. Binnemans, Interpretation of europium(III) spectra, *Coord. Chem. Rev.*, 2015, **295**, 1–45.
26 M. Li, D. Li, M. O'Keeffe and O. M. Yaghi, Topological analysis of metal-organic frameworks with polytopic linkers and/or multiple building units and the minimal transitivity principle, *Chem. Rev.*, 2014, **114**, 1343–1370.
27 N. E. Wong, P. Ramaswamy, A. S. Lee, B. S. Gelfand, K. J. Bladek, J. M. Taylor, D. M. Spasyuk and G. K. H. Shimizu, Tuning Intrinsic and Extrinsic Proton Conduction in Metal–Organic Frameworks by the Lanthanide Contraction, *J. Am. Chem. Soc.*, 2017, **139**, 14676–14683.
28 M. Kumar, L.-Q. Li, J. K. Zaręba, L. Tashi, S. C. Sahoo, M. Nyk, S.-J. Liu and H. N. Sheikh, Lanthanide Contraction in Action: Structural Variations in 13 Lanthanide(III) Thiophene-2,5-dicarboxylate Coordination Polymers (Ln = La–Lu, Except

Pm and Tm) Featuring Magnetocaloric Effect, Slow Magnetic Relaxation, and Luminescence-Lifetime-based Thermometry, *Cryst. Growth Des.*, 2020, **20**, 6430–6452.

29 J. Liu, L. Pei, Z. Xia and Y. Xu, Hierarchical Accordion-like Lanthanide-Based Metal–Organic Frameworks: Solvent-Free Syntheses and Ratiometric Luminescence Temperature-Sensing Properties, *Cryst. Growth Des.*, 2019, **19**, 6586–6591.

30 J. Liu, X. Li, Y. Han, J. Wu, X. Zhang, Z. Wang and Y. Xu, Synergetic Effect of Tetraethylammonium Bromide Addition on the Morphology Evolution and Enhanced Photoluminescence of Rare-Earth Metal-Organic Frameworks, *Inorg. Chem.*, 2020, **59**, 14318–14325.

31 J. Liu, X. Yu, Y. Xu, Y. Zhao and D. Li, Quaternary Ammonium-Mediated Delamination of Europium-Based Metal-Organic Framework into Ultrathin Nanosheets for the Selective Photoelectrochemical Sensing of Fe3+, *Inorg. Chem.*, 2021, **60**, 19044–19052.

32 S. Dang, S. Song, J. Feng and H. Zhang, Microwave-assisted synthesis of nanoscale Eu(BTC)(H_2O)·DMF with tunable luminescence, *Sci. China: Chem.*, 2015, **58**, 973–978.

33 L. Feng, K. Y. Wang, G. S. Day, M. R. Ryder and H. C. Zhou, Destruction of Metal-Organic Frameworks: Positive and Negative Aspects of Stability and Lability, *Chem. Rev.*, 2020, **120**, 13087–13133.

34 K. Binnemans, Lanthanide-Based Luminescent Hybrid Materials, *Chem. Rev.*, 2009, **109**, 4283–4374.

35 Z. Dou, J. Yu, Y. Cui, Y. Yang, Z. Wang, D. Yang and G. Qian, Luminescent metal-organic framework films as highly sensitive and fast-response oxygen sensors, *J. Am. Chem. Soc.*, 2014, **136**, 5527–5530.

36 C. Liu, S. V. Eliseeva, T. Y. Luo, P. F. Muldoon, S. Petoud and N. L. Rosi, Near infrared excitation and emission in rare earth MOFs via encapsulation of organic dyes, *Chem. Sci.*, 2018, **9**, 8099–8102.

37 C. Zhu, S. Kais, X. C. Zeng, J. S. Francisco and I. Gladich, Interfaces Select Specific Stereochemical Conformations: The Isomerization of Glyoxal at the Liquid Water Interface, *J. Am. Chem. Soc.*, 2017, **139**, 27–30.

38 T. N. Nguyen, G. Capano, A. Gladysiak, F. M. Ebrahim, S. V. Eliseeva, A. Chidambaram, B. Valizadeh, S. Petoud, B. Smit and K. C. Stylianou, Lanthanide-based near-infrared emitting metal-organic frameworks with tunable excitation wavelengths and high quantum yields, *Chem. Commun.*, 2018, **54**, 6816–6819.